Materials Physics and Mechanics 47 (2021) 921-936
Research article

Received: March 15, 2021
Accepted: December 6, 2021

# COMBINED EFFECTS OF VISCOUS DISSIPATION AND BROWNIAN MOTION ON TEMPERATURE DISTRIBUTION AND HEAT TRANSFER OF AL2O3/WATER NANOFLUID FLOW THROUGH A POROUS MEDIUM

**Lotfi Bouazizi✉, Said Turki**

National engineering school of Sfax, University of Sfax, B. P. W3038, Sfax, Tunisia.

✉ lot.bouazizi@yahoo.fr

**Abstract.** The combined effect of viscous dissipation and Brownian motion, especially on temperature distribution and heat transfer, has been carried out. Results show that there is an increase in temperature values throughout the field with the increase in the Eckert number $Ec$, this can be proven by the additional source of thermal energy (heat) provided by viscous dissipation in the porous medium, but it makes a decrease in heat transfer. For a lower Darcy number $Da$, the Brownian motion effect is negligible. Without Brownian motion, the averaged Nusselt number reveals an increase when nanoparticles volume fraction $\varphi$ increases. When taking into account the Brownian motion, an increase in the averaged Nusselt number is observed until $\varphi = 0.04$, after that it decreases. This decrease becomes more important by increasing $Ec$.

**Keywords:** nanofluids, viscous dissipation, Brownian motion, temperature distribution, heat transfer, thermal energy

***Acknowledgements****. No external funding was received for this study.*

**Citation:** Bouazizi L., Turki S. Combined effects of viscous dissipation and Brownian motion on temperature distribution and heat transfer of Al2O3/water nanofluid flow through a porous medium // Materials Physics and Mechanics. 2021, V. 47. N. 6. P. 921-936. DOI: 10.18149/MPM.4762021_11.

## 1. Introduction

It is well known that the study of the effect of Brownian motion on flow and heat transfer of nanofluids has been the subject of several studies [1,2,3,4]. However, other research studies have tackled this area in the porous media. The theory of porous flows has many industrial and technological applications such as transport and store energy, electronic cooling, heat exchangers, chemical reactors, and solid matrix nuclear waste disposal, among others. Because of these incessant applications, many researchers have intended the characteristics of nanofluids flow and heat transfer through a porous medium. For example, Nield and Kuznetsov [5] studied symmetric and asymmetric heating configurations for a parallel-plate channel partially filled with a bidisperse porous medium (BDPM). The dependence of the Nusselt number on conductivity ratio, velocity ratio, volume fraction, internal heat exchange parameter, and the position of the porous-fluid interface have been investigated. It has been shown that for asymmetric heating, a singular behaviour of the Nusselt number is satisfactory.

http://dx.doi.org/10.18149/MPM.4762021_11

Teamah et al. [6] carried out a forced convection flow through a pipe partially and completely filled with a porous material for three different cases. The effects of porous material radius as well as Darcy number on local Nusselt number and pressure loss were covered. The results showed that the average Nusselt number of the flow in the pipes with the placement of porous media increased, while the entrance length decreased; there existed a critical value for the external diameter of porous media, and the thermal performance degraded when the external diameter exceeded this value. Hajipour and Dehkordi [7] numerically investigated the combined convective thermal energy transfer of nanofluid flow in a channel, part of which was filled with high porosity medium. Their results proved that the presence of nanoparticles in a porous channel increases the temperature and velocity variation at higher volume fractions. Also, they found that maximum heat transfer is obtained at a higher volume fraction of nanoparticles at the cold wall of the partially filled porous channel. Hatami and Ganji [8] conducted the problem of heat and fluid flow analysis for $SA-TiO_2$ nanofluid in porous media between two coaxial cylinders, by least square. Their results show that an increase in temperature values in the whole domain and an increase in nanoparticle concentration near the inner cylinder wall are caused by increasing the thermophoresis parameter ($Nt$). Hajipour et al. [9] analysed the unsteady two-dimensional mixed convective flow of nanofluids in a vertical channel containing a porous inner layer under the constant wall temperature. Viscous dissipation, Brownian diffusion, and thermophoresis effects were considered in the energy equation. results show that among which filling porous media inside the channel has been verified to be an effective method to improve the utilization rate of heat energy by enhancing heat transfer. Zeeshan et al. [10] studied the $MHD$ flow of nanofluids through a porous medium. Results show that, for both nanofluids, the skin friction coefficient increases with the particle volume fraction, and the skin friction and heat transfer rate of nanofluids decrease with an increase in the magnetohydrodynamic parameter. Aaiza et al. [11] analyzed the radiative heat transfer in mixed convection $MHD$ flow of different shapes of $Al_2O_3$ in $EG$-based nanofluid in a channel filled with a saturated porous medium. Results show that, under the effect of an increase of viscosity and thermal conductivity of nanofluid, the velocity decreases with the increase of volume fraction of nanoparticles. On the other hand, the velocity of water-based nanofluid is concluded important than $EG$-based nanofluid because the viscosity of base fluid affects the Brownian motion of the nanoparticles. Subhania and Nadeem [12] studied the behavior of a three-dimensional micropolar nanofluid over an exponentially stretching surface in a porous medium. Three different nanoparticles, namely alumina, titania, and copper are compared taking water as the base fluid. Results show that the microrotation increases the rate of the heat transfer of the nanofluid due to the decreasing impact on the skin friction. On the other hand, an increase in the nanoparticles volume fraction leads to an increase in the coefficient of friction, as well as a decrease in the local Nusselt number. Nojoomizadeh et al. [13] examined the fluid flow and heat transfer of a nanofluid, consisting of the functionalized multi-walled carbon nanotubes suspended in water, in a two-dimensional microchannel filled by porous media. Their results demonstrate that, at a lower Reynolds number, the local Nusselt number was reduced quickly. On the other hand, the slip coefficient is assumed to be one of the effective parameters of the increase in the local Nusselt number, notably for higher Reynolds numbers and lower Darcy numbers. A.S. Dogonchi et al. [14] studied numerically the effect of Brownian motion on the Magnetic nanofluid natural convection in the porous enclosure. The results show that the heat transfer increases with increasing Rayleigh number, Darcy number, and inclination angle of the magnetic field. In addition, the location of the maximum value of the local Nusselt number approaches the bottom of the adiabatic wall with increasing Rayleigh number. Mishra and Mathur [15] analyzed the two-dimensional time-independent flow of non-Newtonian Williamson nanofluid over a stretching surface through a porous medium. The results show

that the Brownian motion and the thermophoretic parameters retard both the particle concentration profiles and the mass transfer rate of the nanofluid. On the other hand, the rate of shear stress increases with an increase in the magnetic parameter but retards the heat transfer.

The literature on this subject is vast and considering these factors and deriving inspiration from the previously mentioned works in the field of nanofluids, there is no research that has undertaken the temperature distribution and the heat transfer of nanofluids through a porous medium, taking into account the viscous dissipation and the Brownian motion. Moreover, the two-phase-flow heat transfer effect of the horizontal channel is better, so this paper designed an exchange of the thermal heat flux between the flow and the horizontal walls of the channel. On the other hand, transport phenomena in porous media in horizontal channels are of continuing interest by many researchers in the literature because of their significant applications in the engineering and biomedical sectors. Such applications include thermal management of high heat flux electronic devices, thermal insulation in buildings, petroleum industries, drug delivery, transport in biological tissues, and porous scaffold for tissue engineering. So, there is a physical reason to investigate the topic of the current article in order to contribute to the combined effect of viscous dissipation and Brownian motion on temperature distribution and heat transfer of $Al_2O_3$-water nanofluid through porous medium over a horizontal channel. The viscosity of nanofluid is based on Brownian motion. Also, the effects of some parameters such as viscous dissipation, Brownian motion, Darcy and Reynolds number, and nanoparticles volume fraction on temperature profile and heat transfer are investigated.

## 2. Governing equations

Figure 1 shows a schematic of the geometry and related boundary conditions. The porous medium layer characterized by permeability $K_p$ and height $H$. The main effective parameters involved in the problem were dimensionless numbers of Darcy $Da$, Eckert $Ec$, Reynolds $Re$, Brownian motion parameters, and nanoparticles volume fraction $\varphi$.

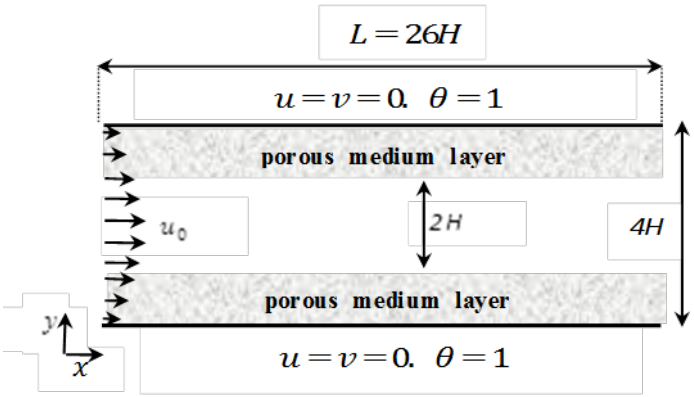


**Fig. 1.** Configuration definition

The dimensionless of the continuity, momentum, and thermal energy equations governing the laminar flow are given below in the following conservative form:

$$div(\boldsymbol{V}) = 0, \tag{1}$$

$$\frac{\partial u}{\partial \tau} + div(\boldsymbol{J_u}) = -\frac{\rho_f}{\rho_{nf}}\frac{\partial P}{\partial x} - \frac{u}{Re\,Da}, \boldsymbol{J_u} = u\boldsymbol{V} - \frac{1}{Re}\frac{\mu_{nf}}{\mu_f}\frac{\rho_f}{\rho_{nf}}\boldsymbol{grad}(u), \quad (2)$$

$$\frac{\partial v}{\partial \tau} + div(\boldsymbol{J_v}) = -\frac{\rho_f}{\rho_{nf}}\frac{\partial P}{\partial y} - \frac{v}{Re\,Da}, \boldsymbol{J_v} = v\boldsymbol{V} - \frac{1}{Re}\frac{\mu_{nf}}{\mu_f}\frac{\rho_f}{\rho_{nf}}\boldsymbol{grad}(v), \quad (3)$$

$$\frac{\partial \theta}{\partial \tau} + div(\boldsymbol{J_\theta}) = \frac{Ec}{Re\,Da}(u^2 + v^2), \boldsymbol{J_\theta} = \theta\boldsymbol{V} - \frac{1}{Re.Pr}\frac{\alpha_{nf}}{\alpha_f}\boldsymbol{grad}(\theta). \quad (4)$$

The effective density ($\rho_{nf}$), the thermal expansion coefficient ($\beta_{nf}$) and heat capacitance $(\rho Cp)_{\mathrm{nf}}$ of the nanofluid are defined as (Khanafer et al. [16]):

$$\rho_{nf} = (1-\varphi)\rho_f + \varphi\rho_s, \quad (5)$$

$$\beta_{nf} = (1-\varphi)\,\beta_f + \varphi\beta_s, \quad (6)$$

$$(\rho Cp)_{nf} = (1-\varphi)\,(\rho Cp)_f + \varphi(\rho Cp)_s. \quad (7)$$

The thermos-physical properties of water and $Al_2O_3$ nanoparticles are shown in Table 1.

Vajjha et al. [17] proposed an expression for the effective thermal conductivity, composed of the particle's conventional static part and a Brownian motion part.

$$k_{nf} = k_{static} + k_{Brownian}. \quad (8)$$

The $k_{static}$ is the static thermal conductivity based on Maxwell classical correlation.

$$k_{static} = k_f\left[\frac{(k_s+2k_f)-2\varphi(k_f-k_s)]}{(k_s+2k_f)+\varphi(k_f-k_s)}\right], \quad (9)$$

where $k_f$ and $k_s$ are the thermal conductivities of the base fluid and the solid particles respectively. The thermal conductivity due to the Brownian motion is given by Vajjha et al. [18] as:

$$k_{Brownian} = 5\times10^4\beta\varphi\rho c_{p,f}\sqrt{\frac{KT}{\rho_{np}\mathrm{d}_{np}}}f(T,\varphi), \quad (10)$$

where

$$f(T.\varphi) = (2.8217\times10^{-2}\varphi + 3.917\times10^{-3})\left(\frac{T}{T_0}\right) + (-3.0669\times10^{-2}\varphi - 3.91123\times10^{-3}), \quad (11)$$

$K$ is the Boltzmann constant, $T$ is the fluid temperature, and $T_0$ is the reference temperature.

Table 1. The thermo-physical properties of water and $Al_2O_3$ nanoparticles at $T = 300K$ (Incropera and DeWitt [13])

| Thermo-physical properties | Water | $Al_2O_3$ |
|---|---|---|
| Density, ρ ($kg/m^3$) | 998.2 | 3970 |
| Specific heat, $c_p$ ($J/kg.K$) | 4182 | 765 |
| Thermal conductivity, k ($W/m\,K$) | 0.6 | 40 |
| Dynamic viscosity, μ ($Ns/m^2$) | 0.001003 | -- |
| Thermal expansion, β ($1/K$) | 207E-06 | 5.80E-06 |

The effective viscosity of nanofluids based on Brownian motion has been developed by Masoumi et al. [19]. It is expressed as follow:

$$\mu_{nf} = \mu_f + \frac{\rho_{np}V_B d_{np}^2}{72C\delta}, \quad (12a)$$

in which:

$$V_B = \frac{1}{\mathrm{d}_{np}}\sqrt{\frac{18KT}{\pi\rho_{np}\mathrm{d}_{np}}}, \quad (12b)$$

$$\delta = \sqrt[3]{\frac{\pi}{6\varphi}}\,\mathrm{d}_{np}, \quad (12c)$$

$$C = \mu_f^{-1}\left[\left(c_1\mathrm{d}_{np} + c_2\right)\varphi + \left(c_3\mathrm{d}_{np} + c_4\right)\right], \quad (12d)$$

where: $c_1 = -0.000001133$, $c_2 = -0.000002771$, $c_3 = 0.00000009$, $c_4 = -0.000000393$; $\mu_{nf}$ and $\mu_f$ are the viscosity of nanofluid and base fluid respectively; $d_{np}$ is the nanoparticle diameter and $\varphi$ is the nanoparticle volume fraction; $V_B$ is the Brownian velocity of nanoparticles, it is defined by [19].

The $\beta$ equation for $Al_2O_3$ particles is expressed as it is given by Vajjha and Das [20] as: $\beta = 8.4407(100\varphi)^{-1.07304}$ for $1\% \leq \varphi \leq 10\%$ and $298\ K \leq T \leq 363\ K$.

The authors of the work [21] further investigated laminar nanofluid flow in micro heat sinks using the effective nanofluid thermal conductivity model that they have established. It includes the effects of nanoparticle size, nanoparticle volume fraction, and temperature dependence as well as properties of the base fluid and the nanoparticle subject to Brownian motion. For the effective viscosity, they proposed:

$$\mu_{nf} = \mu_{static} + \mu_{Brownian} = \mu_{static} + \frac{k_{Brownian}}{k_f} \times \frac{\mu_f}{Pr}, \quad (13)$$

where $\mu_{static} = \frac{\mu_f}{(1-\varphi)^{2.5}}$ is the viscosity of the nanofluid, as given originally by Brinkman [22] and $Pr$ the value of Prandtl number which maintained at 6.2.

In the above equations, the space coordinates, time, velocities, and pressure are normalized with the porous medium thickness $H$, the characteristic time $\frac{H}{u_0}$, the maximum velocity of the channel inlet $u_0$, and the characteristic pressure $\rho_f u_0^2$ respectively. The dimensionless variable $\theta$ was defined as: $\theta = \frac{(T-T_c)}{(T_h-T_c)}$ where $T_c$ and $T_h$ are cold and hot temperatures, respectively.

***Dimensionless boundary conditions:***

- *at the inlet:* $u = \frac{y}{4}(4-y)$, $v = 0$ and $\theta = 0$,
- *at the top and bottom walls:* $u = 0, v = 0$ and $\theta = 1$,
- *at the outlet:* Convective boundary condition (CBC) for $u$, $v$ and $\theta$ is used.

The $CBC$ is formulated as: $\frac{\partial \phi}{\partial t} + u_{av}\frac{\partial \phi}{\partial x} = 0$.

Here $\phi = u$, $v$ or $\theta$ and $u_{av}$ is the average channel inlet velocity. As reported by Sani and Gresho [23] and Sohanker et al. [24], $CBC$ predicts correctly the flow at the exit especially when vortices leave the domain.

The thermal heat flux exchanged between the flow and the horizontal walls of the channel step are characterized by the space averaged Nusselt number evaluated as follows:

$$Nu_{av} = \frac{1}{L}\int_0^L Nu(x)dx, \quad (14)$$

where $Nu(x)$ is the local Nusselt number, computed with the following equation (Abu-Nada [25]):

$$Nu(x) = \frac{1}{\theta_b(x)-1}\frac{k_{nf}}{k_f}\frac{\partial \theta}{\partial y}\Big|_{wall}, \quad (15)$$

$\theta_b(x)$ is the bulk temperature, calculated using the velocity and the temperature distribution with the equation:

$$\theta_b(x) = \frac{\int_0^1 u\theta dy}{\int_0^1 u dy}. \quad (16)$$

## 3. Solution procedures

The combined equations, governing laminar flow, are solved using a Patankar finite volume method [26]. To prevent the occurrence of checkerboard pressure fields, the control volume cells for the velocity components are staggered with respect to the main control volume cells. The convection terms in Equations (2-4) were discretized using the hybrid scheme, while the diffusion terms were discretized using second-order central scheme. The SIMPLER algorithm

was applied to solve the pressure-velocity coupling in conjunction with an alternating direction implicit scheme to perform the time evolution.

Our computations were achieved using $249 \times 93$ nonuniform meshes with a variable grid size $0.01 \leq \Delta x \leq 0.4$ and $0.01 \leq \Delta y \leq 0.05$. (More details about the validity of the computational code and the grid used in this work are available in Bouazizi et al. [27]).

## 4. Results and discussions

The main objective of the present study is to examine the temperature repartition and heat transfer of $2D$ laminar and forced convective flow in a horizontal channel using $Al_2O_3 -$ water nanofluid through a porous medium by considering the Brownian motion and the viscous dissipation.

Computations were carried out for a flow under temperature difference $\Delta T$ up to 35. Different Darcy, Eckert, and Reynolds numbers and volume fractions of nanoparticles ranging respectively from $Da = 10^{-4}$ to $10^3$, $Ec = 0$ to 1, $Re = 150$ to 250, and $\varphi = 1\%$ to 6%, have been considered to show their effects on several parameters such us velocity, streamlines, temperature field, and Nusselt number.

Figure 2 shows the instantaneous streamline contours for different Darcy numbers at $Re = 150$, $\varphi = 0.04$, and $\mathrm{Ec} = 0$. It should be pointed out that the fluid is identified to a porous medium of the great value of Darcy number ($Da \geq 10^{-1}$).

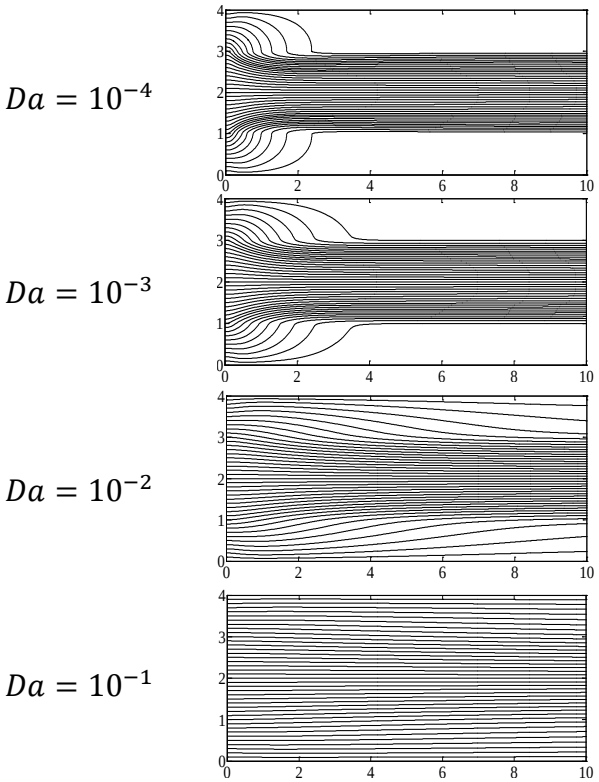


**Fig. 2.** the instantaneous streamline contours for different Darcy number

The velocity profile for different Darcy numbers at $X = 0.98$ is shown in Fig. 3b. It is found that the velocity profile extends further towards the fluid flow at the center of the channel as $Da$ decreases and a shorter entrance length is expected in the porous media. However, increasing the Darcy number (i.e., the permeability inside the porous medium) leads to a nonlinear distribution of the velocity. For a lower Darcy number, the velocity profile is independent of the transverse distance Y, and the flow experiences larger resistance, and an adverse pressure gradient is developed between free fluid and porous medium at

$Da = 0.0001$ and, correspondingly, the shear stress at the wall changes its sign causing vortices. The vortices are the origin of the inverse behavior of the velocity is shown at the center of the channel. On the other hand, Fig. 3a illustrates the dimensionless temperature profile inside the channel for $Da = 0.0001$, $0.01$, and $1$. These profiles show that the temperature values at the walls and the center of the channel have maximum and zero values, respectively. The temperature difference between the wall and the fluid decreases in the porous medium with the decrease in $Da$ numbers. The results in Fig. 4 show that, in the region near the channel walls, the isotherms become more and more compact by increasing Darcy number. Also, a small Darcy number features low permeability in the porous medium and thus induces smaller convection in a more restrictive medium.

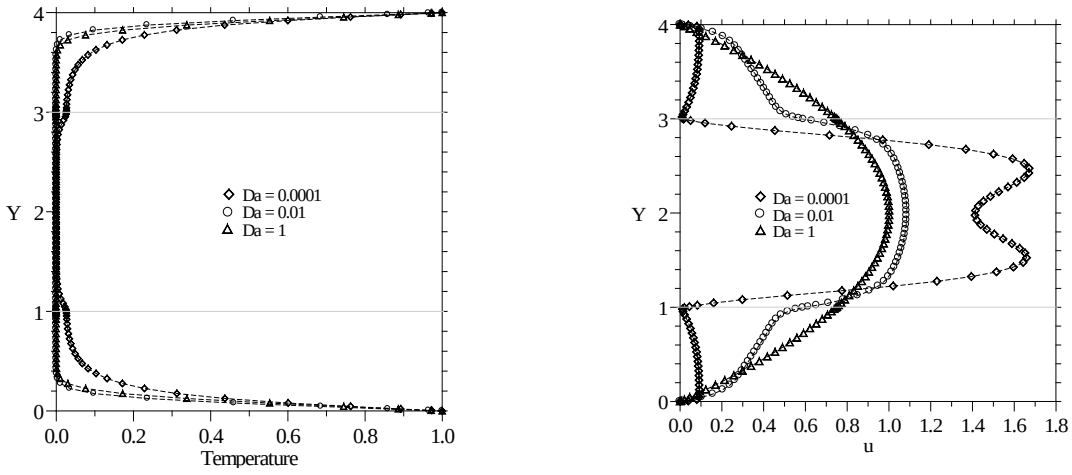


**Fig. 3.** Effect of Darcy number for $Ec = 0$, $Re = 150$ and $\varphi = 0.04$ at $X = 0.98$, on (a) temperature distribution and (b) velocity distribution

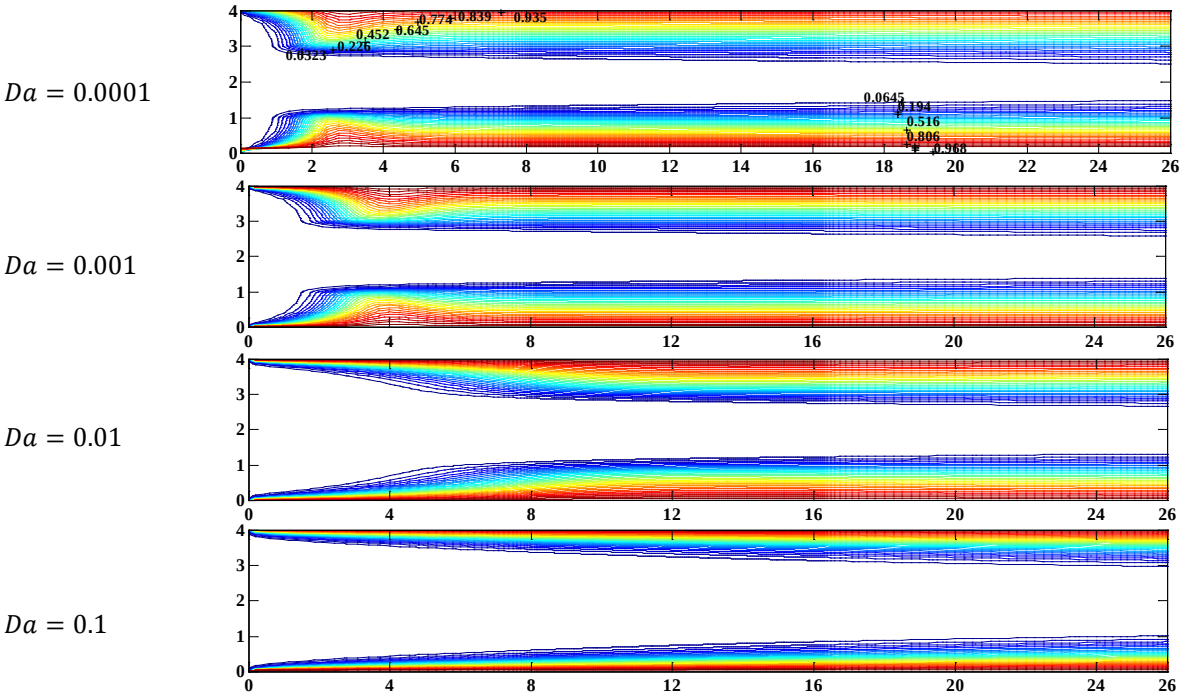


**Fig. 4.** Effect of Darcy number on isothermal lines contours for $Ec = 0$, $Re = 150$ and $\varphi = 0.04$

Figures 5-7 illustrate the effect of the viscous dissipation (Eckert number $Ec$) on the temperature profiles and Nusselt number respectively. An increase in the value of the Eckert number has the tendency to increase the fluid temperature and decrease the heat transfer, and so, to increase the thermal buoyancy effects. Therefore, viscous dissipation in a flow through a porous medium is beneficial for gaining the temperature. Physically, this behavior is observed because in the presence of viscous dissipation, heat energy is stored in the fluid, and there is a more significant generation of heat along with the porous medium. Also, it is evident from these figures that the effect of the viscous dissipation parameter is to enhance the temperature distribution.

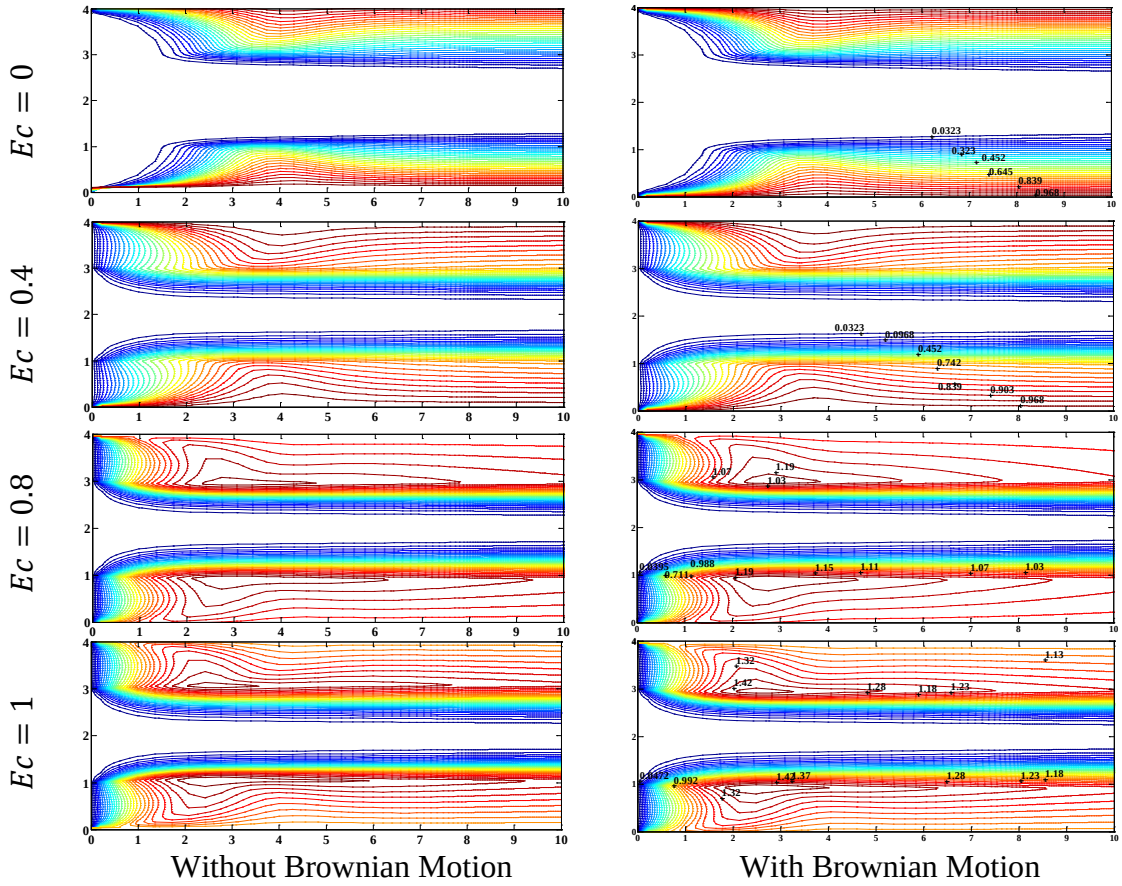


**Fig. 5.** Effect of viscous dissipation ($Ec$) on isothermal lines contours for $Da = 0001$, $Re = 150$, and $\varphi = 0.04$

Figure 7 shows that for a small Darcy number ($Da = 0.001$), the Brownian Motion effect is negligible, that because of the difficulty of the movement of the fluid in the porous medium. On the other hand, it can be deduced that a high Eckert number ($Ec$) causes a considerable increase in temperature. This outbreak of temperature is due to the additional source of thermal energy (heat) provided by viscous dissipation in the porous medium. On the other hand, this temperature rise is happening due to the effect of nanoparticles' heat capacity. This can be verified, indeed, the friction in the porous medium due to nanofluid viscosity causes more heat, and as a result the nanofluid temperature increases.

By observing the isothermal line contours as depicted in Fig. 5, the thermal boundary layer thickness increases by increasing $Ec$, resulting in storage of thermal energy in the fluid. The effect of Brownian motion and viscous dissipation on the Nusselt numbers are presented in Fig. 6. By increasing $Da$, the wall's heat is dispersed in the direction of the center of the channel, warming up the solid matrix. Thus, the fluid particles gain heat and they heat up

which leads to a decrease in the temperature gradient due to the increase of the thickness of the thermal boundary layer, and therefore a reduction in heat transfer. Indeed, for $Da = 10^{-3}$ and when taking into account the Brownian motion, we observe a decrease of the heat transfer by 94 %, 92 %, and 50 %, for $Ec = 1$, $Ec = 08$, and $Ec = 0.4$, respectively. On the other hand, there is an increase of 6% for $Ec = 0$ (absence of viscous dissipation). For $Da$ very low, the generation of heat has no role in the evolution of the temperature field in the porous layer because the inertia forces generated by the solid matrix are negligible. On the other hand, figures show that for a Darcy number important, heat transfer begins to increase and asymptotically approaches the corresponding value without a porous medium.

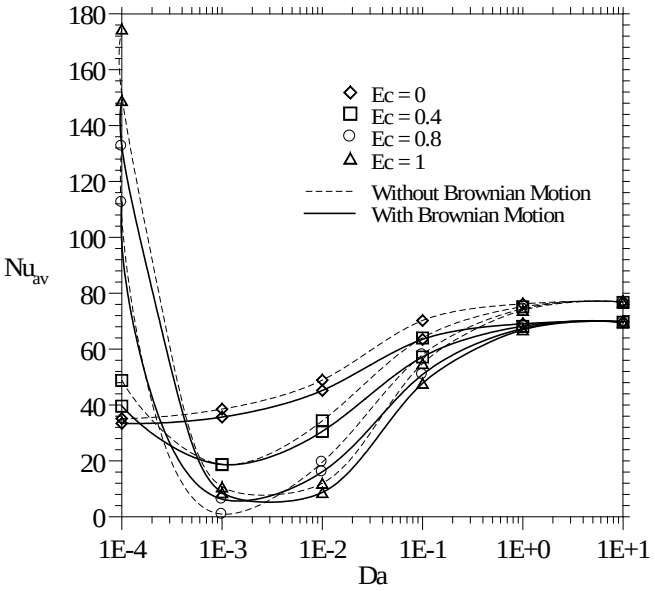


**Fig. 6.** Effect of viscous dissipation ($Ec$) on the variation of $Nu_{av}$ with $Da$

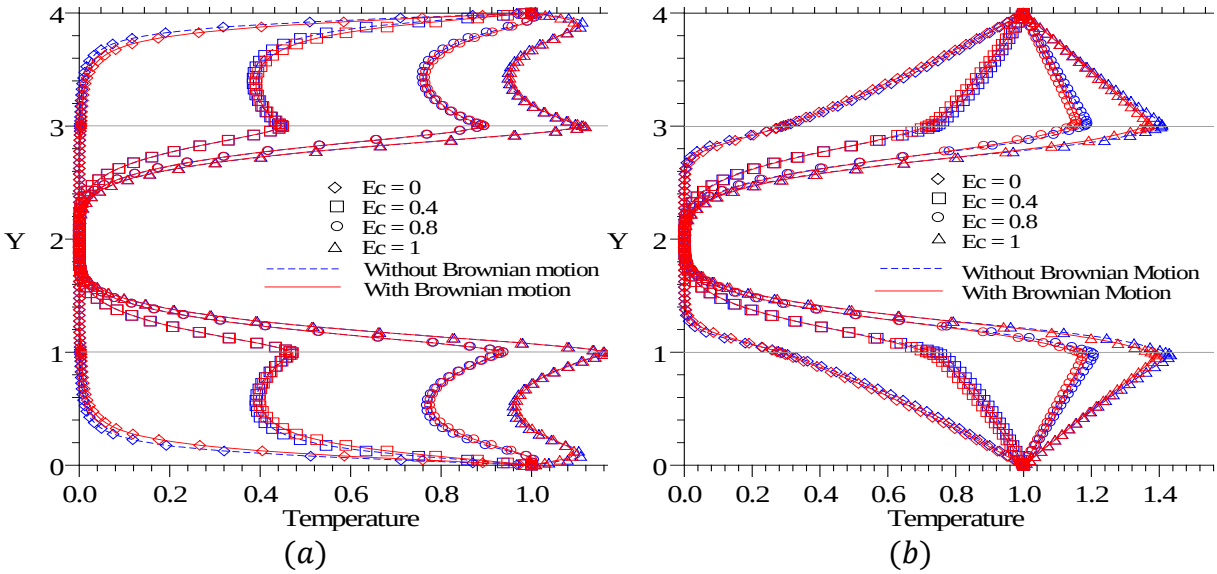


**Fig. 7.** Effect of viscous dissipation ($Ec$) for $Da = 0.001$, $\varphi = 0.04$ and $Re = 150$ on temperature distribution, at (a) $X = 0.98$ and (b) $X = 5.075$

The effects of the viscous dissipation and Brownian motion on the heat transfer are shown in Fig. 8. A close glance at Fig. 8, without Brownian motion, the averaged Nusselt number reveals an increase when increasing the nanoparticles volume fraction. With Brownian motion, the increase is until $\varphi = 0.04$, then it starts to decrease. This decrease

becomes more important by increasing $Ec$. For example, a reduction in the vicinity of 0.85%, 20%, 50%, and 91%, for $Ec = 0.2$, $Ec = 0.4$, $Ec = 0.6$, and $Ec = 0.8$, respectively, when $\varphi$ pass from 0.04 to 0.06. Furthermore, as shown in this figure, the heat transfer decreases in the presence of viscous dissipation by considering the Brownian motion which represents one of the key heat transfer mechanisms in nanofluids [1,28]. By considering the Brownian motion, for $\varphi = 0.05$, this decreases in heat transfer increases from 15% to 27% when $Ec$ passes from 0 to 1, compared with that in the case of disregarding the Brownian motion. In effect, taking into account the Brownian motion, the temperature increases (see Fig 9b). Again, this is happened due to the effect of nanoparticles' heat capacity. It is clear that the concentration of nanofluid decreases with the presence of the Brownian motion, which can be justified according to the temperature of boundaries and the temperature increase of the flow field. Increases in the value of the Eckert number have the tendency to increase the rate of decrease of the solute concentration, which is proved by the decreases of the heat transfer rate as $Ec$ exceeds 0.4.

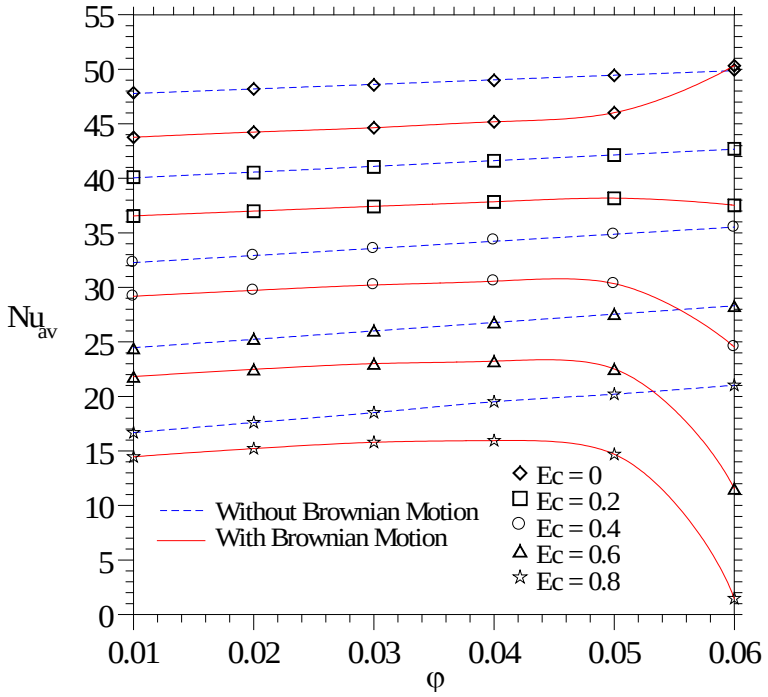


**Fig. 8.** Effect of viscous dissipation and Brownian motion on variation of $Nu_{av}$ with $\varphi$

Figure 9 shows the effect of viscous dissipation on a temperature profile for two values of nanoparticles volume fraction ($\varphi = 0.05$ and $\varphi = 0.06$), with and without Brownian Motion. As it can be seen, in presence of Brownian motion and by considering the Eckert number (Fig. 9b), an increase of temperature magnitude inside the porous medium is caused. Moreover, with the increase of nanoparticles volume fraction the maximum temperature point shifts with the flow. This change in direction of temperature for $\varphi = 0.06$ represents changes in $\langle \overline{Nu}_T \rangle$ sign, see Fig 8. Figure 10 confirms this result where we have plotted the isotherm contours for $\varphi = 0.06$. It is also shown that, with Brownian motion for $Ec = 0.4$, the temperature contours are steeper near the walls of the channel. Therefore, a reduction of the temperature gradient and a reduction of the heat transfer are achieved for $\varphi = 0.06$.

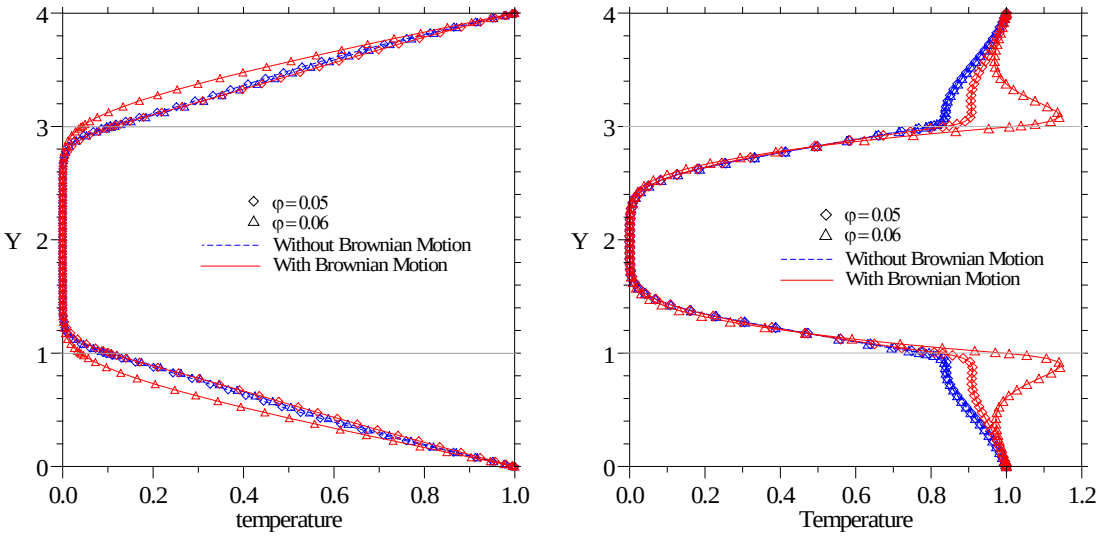


**Fig. 9.** Effect of nanoparticles volumes fraction $\varphi$ and Brownian motion for $Da = 0.01$ and $Re = 150$, at $X = 8$, on temperature distribution, (a) $Ec = 0$ and (b) $Ec = 0.4$

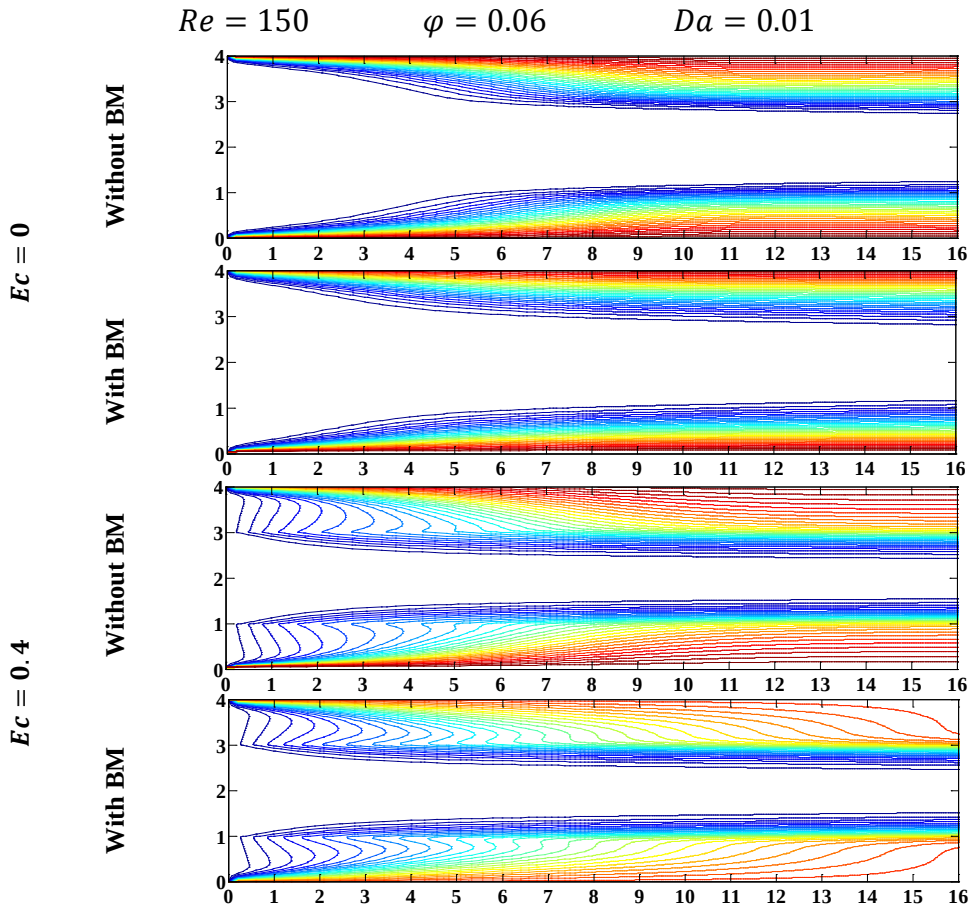


**Fig. 10.** Effect of viscous dissipation ($Ec$) on isothermal lines contours for $Da = 0.01$, $Re = 150$, and $\varphi = 0.06$

The effect of the Brownian Motion on the temperature distribution for three Reynolds numbers 150, 190, and 230, is shown in Fig. 11 for two Darcy numbers ($Da = 0.001$ and $Da = 0.01$). Figure 11a demonstrates that the temperature is high in the porous medium (lower $Da$ values). This outcome is due to the increase of a viscous dissipation effect using a

porous medium with low permeability. For a small Darcy number ($Da$), the Reynolds number effect is negligible. The Reynolds number effect increases with increasing $Da$, and therefore fluid gradient temperatures are seen to increase, especially by considering Brownian motion (mainly in the porous medium). Moreover, the distribution of the Nusselt number at the channel walls reveals an enhancement by increasing Reynolds number (see Fig. 12), which remains superior without Brownian motion. It can be seen as an important enhancement, especially for $Da = 0.01$. For example, for $Re = 250$, an increase in the vicinity of 38% and 48% for $Da = 0.001$ and $Da = 0.01$, respectively. This behavior is explained by looking at Eq. (15) which the expression of the Nusselt number consists of three terms which are the term for the temperature difference between the wall and the fluid bulk temperature (i.e. $1/(\theta_b - 1)$), the term for thermal conductivity ratio (i.e. $k_{nf}/k_f$) and the term for the temperature gradient at the wall (i.e. $d\theta/dy$).

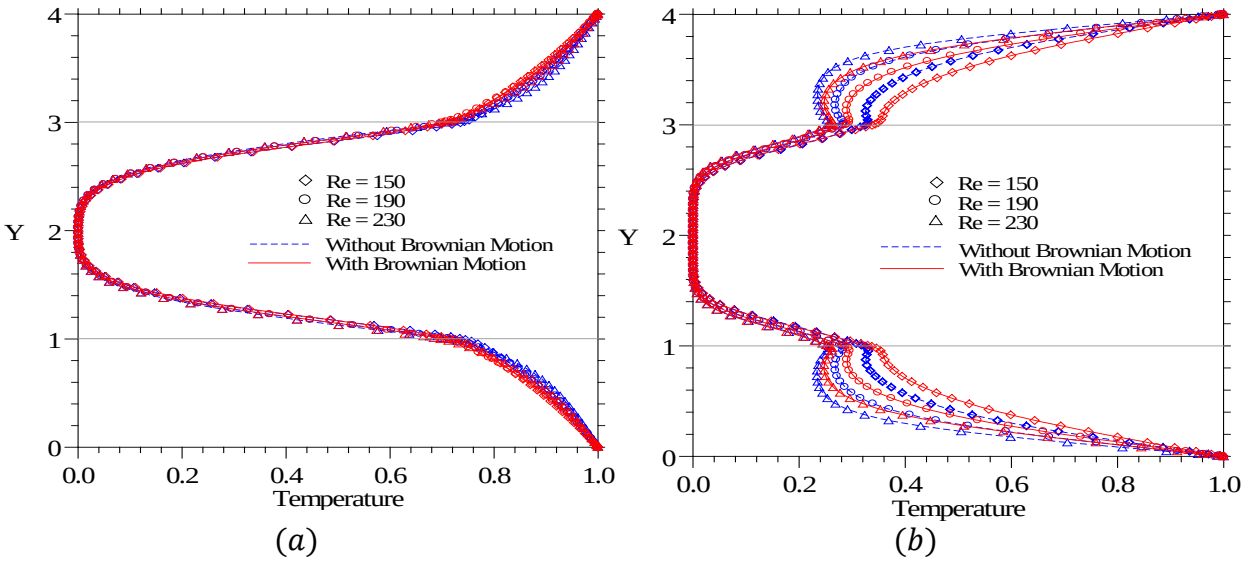


**Fig. 11.** Effect of Reynolds number ($Re$) on isothermal lines contours for $Ec = 0.4$ and $\varphi = 0.04$ at $X = 5.075$, (a) $Da = 0.001$ and (b) $Da = 0.01$

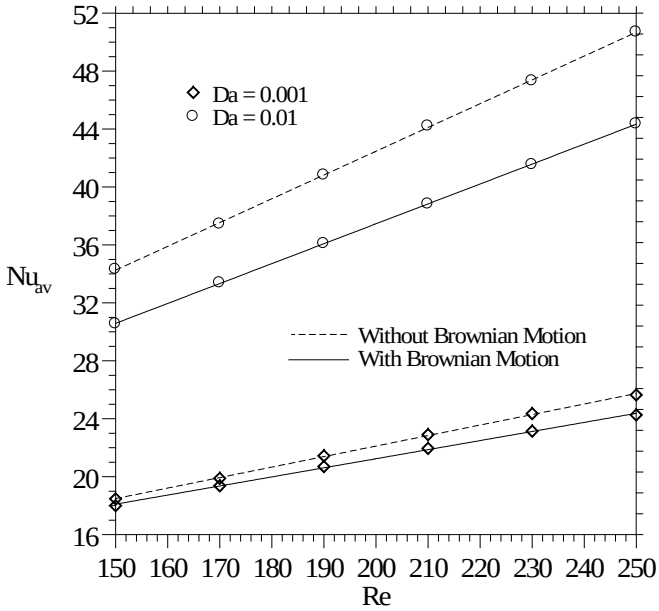


**Fig. 12.** Effect of Brownian motion and Darcy number on variation of $Nu_{av}$ with $Re$

## 5. Conclusion

The influence of viscous dissipation and Brownian motion on forced convection flow in the horizontal channel through a porous medium has been numerically investigated. The effects of physical parameters including Eckert number, Darcy number, Reynolds number, and Brownian motion on the profiles of velocities, temperature, and heat transfer are examined. The following conclusions were drawn in our study:

1. The viscous dissipation effect increases with decreasing Darcy number. As a consequence, the local fluid temperatures increase. The viscous dissipation provides a thermal energy (heat) source downstream and thus changes the nature of the fully developed temperature distribution and the heat transfer.
2. For a lower Darcy number, the Brownian motion effect is negligible, that because of the difficulty of the movement of the fluid in the porous medium.
3. Without Brownian motion, the averaged Nusselt number reveals an increase when $\varphi$ increases. With Brownian motion, the increasing of the Nusselt number is until $\varphi = 0.04$, then it starts to decrease, this decrease becomes more important by increasing $Ec$.
4. The distribution of the Nusselt number at the channel walls reveals an enhancement by increasing the Reynolds number, which remains higher without Brownian motion.
5. The Nusselt number has a direct relationship with Eckert number, nanoparticle volume fraction, and Reynolds number.

## NOMENCLATURE

| | | | |
|---|---|---|---|
| $C_p$ | specific heat at constant pressure $(kJ.kg^{-1}.K^{-1})$ | $v$ | dimensionless $y$ component of velocity |
| $h$ | convection heat transfer coefficient $(W.m^{-2}.K^{-1})$ | $x$ | dimensionless horizontal coordinate |
| $H$ | downstream channel height $(m)$ | $y$ | dimensionless vertical coordinate |
| $k$ | thermal conductivity $(W.m^{-1}.K^{-1})$ | ***Greek symbols*** | |
| $K$ | Boltzmann constant $(J\,K^{-1})$ | $\alpha$ | thermal diffusivity $(m^2.s^{-1})$ |
| $K_p$ | Permeability of the porous media $(m^2)$ | $\beta$ | coefficient of thermal expansion $(K^{-1})$ |
| $L$ | length of the channel $(m)$ | $\phi$ | transport quantity |
| $Nu$ | Nusselt number | $\varphi$ | nanoparticle volume fraction |
| $Nu_{av}$ | Space-average Nusselt number | $\nu$ | kinematic viscosity $(m^{-2}.s^{-1})$ |
| $P$ | dimensionless pressure | μ | dynamic viscosity $(kg.m^{-1}.s^{-1})$ |
| $p$ | pressure $(N.m^{-2})$ | $\theta$ | dimensionless temperature |
| $Pe$ | Peclet number $(= Re.Pr)$ | $\rho$ | density $(kg.m^{-3})$ |
| $Pr$ | Prandtl number $(= \frac{\nu_f}{\alpha_f})$ | $\tau$ | time dimensionalized |
| $qw$ | heat flux at the wall $(W.m^{-2})$ | ***Subscripts*** | |
| $Da$ | Darcy number $(= \frac{K_p}{H^2})$ | $av$ | average value |
| | | $b$ | bulk value |
| $Ec$ | Eckert number $(= \frac{u_\infty^2}{Cp(T_w - T_\infty)})$ | $nf$ | Nanofluid |
| $Re$ | Reynolds number $(= \frac{\rho_f.u_0.H}{\mu_f})$ | $f$ | Fluid |
| | | $s$ | Solid |
| $T$ | dimensionaltemperature $(K)$ | $w$ | Wall |
| $t$ | time non-dimensionalized $(s)$ | $wc$ | cold wall |
| $x$ | mean channel inlet velocity | $wh$ | hot wall |
| $u_0$ | maximum velocity of the channel inlet | $av$ | average value |
| $u$ | dimensionless component of velocity | $\infty$ | Main flow |

## References

[1] Jang SP, Choi Stephen US. Role of Brownian motion in the enhanced thermal conductivity of nanofluids. *Appl. Phys. Lett.* 2004;84(21): 4316-4318.

[2] Sheikholeslami M, Ganji DD. Nanofluid flow and heat transfer between parallel plates considering Brownian motion using DTM. *Computer Methods in Applied Mechanics and Engineering.* 2015;283(1): 651-663.

[3] Bouazizi L, Turki S. Effect of Brownian motion on flow and heat transfer of nanofluids over a backward-facing step with and without adiabatic square cylinder. *Thermophys Aeromech.* 2018;25(3): 445-460.

[4] Abdelmalek Z, Hussain A, Bilal S, El-Sayed MS, Thounthong P. Brownian motion and thermophoretic diffusion influence on thermophysical aspects of electrically conducting viscoinelastic nanofluid flow over a stretched surface. *Journal of Materials Research and Technology.* 2020;9(5): 11948-11957.

[5] Kuznetsov AV, Nield DA. Forced convection in a channel partly occupied by a bidisperse porous medium: Asymmetric case. *International Journal of Heat and Mass Transfer.* 2010;53(23-24): 5167-5175.

[6] Mohamed AT, Wael ME, Mohamed MKD. Numerical simulation of laminar forced convection in horizontal pipe partially or completely filled with porous material. *International Journal of Thermal Sciences.* 2011;50(8): 1512-1522.
[7] Mastaneh H, Asghar MD. Analysis of nanofluid heat transfer in parallel-plate vertical channels partially filled with porous medium. *International Journal of Thermal Sciences.* 2012;55: 103-113.
[8] Hatami M, Ganji DD. Heat transfer and flow analysis for SA-TiO2 non-Newtonian nanofluid passing through the porous media between two coaxial cylinders. *Journal of Molecular Liquids.* 2013;188: 155-161.
[9] Mastaneh H, Asghar MD, Jamshidi, S. Numerical Investigation of Nanofluid Mixed-Convection Flow in the Entrance Region of a Vertical Channel Partially Filled with Porous Medium. *Heat Transfer-Asian Research.* 2014;43(7): 607-627.
[10] Zeeshan A, Ellahi R, Hassan M. Magnetohydrodynamic flow of water/ethylene glycol based nanofluids with natural convection through a porous medium. *The European Physical Journal Plus.* 2014;129: 261-270.
[11] Gul A, Khan I, Shafie S. Energy transfer in mixed convection MHD flow of nanofluid containing different shapes of nanoparticles in a channel filled with saturated porous medium. *Nanoscale Res Lett.* 2015;10: 490.
[12] Subhania M, Nadeem S. Numerical analysis of 3D micropolar nanofluid flow induced by an exponentially stretching surface embedded in a porous medium. *The European Physical Journal Plus.* 2017;132: 441.
[13] Nojoomizadeh M, D'Orazio A, Karimipour A, Afrand M, Goodarzi M. Investigation of permeability effect on slip velocity and temperature jump boundary conditions for FMWNT/Water nanofluid flow and heat transfer inside a microchannel filled by a porous media. *Physica E: Low-dimensional Systems and Nanostructures.* 2018;97: 226-238.
[14] Dogonchi AS, Seyyedi MS, Hashemi-Tilehnoee M, Chamkha AJ, Ganji DD. Investigation of natural convection of magnetic nanofluid in an enclosure with a porous medium considering Brownian motion. *Case Studies in Thermal Engineering.* 2019;14: 100502.
[15] Mishra SR, Mathur P. Williamson nanofluid flow through porous medium in the presence of melting heat transfer boundary condition: semi-analytical approach. *Multidiscipline Modeling in Materials and Structures.* 2020;17(1): 19-33.
[16] Khanafer K, Vafai K. Lightstone M. Buoyancy-driven heat transfer enhancement in a two-dimensional enclosure utilizing nanofluids. *International Journal of Heat and Mass Transfer.* 2003;46(19): 3639-3653.
[17] Incropera FP, DeWitt D.P. *Fundamentals of Heat and Mass Transfer.* 5th ed. 2007.
[18] Vajjha RS, Das DK, Kulkarni DP. Development of new correlations for convective heat transfer and friction factor in turbulent regime for nanofluids. *International Journal of Heat and Mass Transfer.* 2010;53(21): 4607-4618.
[19] Masoumi N, Sohrabi N, Behzadmehr A. A new model for calculating the effective viscosity of nanofluids. *J. Phys. D. Appl. Phys.* 2009;42(5): 055501.
[20] Vajjha RS, Das DK. Experimental determination of thermal conductivity of three nanofluids and development of new correlations. *International Journal of Heat and Mass Transfer.* 2009;52(21-22): 4675-4682.
[21] Koo J, Kleinstreuer C. A new thermal conductivity model for nanofluids. *Journal of Nanoparticle Research.* 2004;6(6): 577-588.
[22] Brinkman HC. The viscosity of concentrated suspensions and solutions. *Journal of Chemical Physics*. 1952;20(4): 571-581.
[23] Sani RL, Gresho PM. Résumé and remarks on the open boundary condition minisymposium. *Int. J. Num. Meth. Fluids.* 1994;18(10): 983-1008.

[24] Sohankar A, Norberg C, Davidson L. Low-Reynolds number flow around a square cylinder at incidence: Study of blockage, onset of vortex shedding and outlet boundary condition. *International Journal for Numerical Methods in Fluids.* 1998;26(1): 39-56.
[25] Abu-Nada E. Application of nanofluids for heat transfer enhancement of separated flows encountered in a Backward Facing Step. *International Journal of Heat and Fluid Flow.* 2008;29(1): 242-249.
[26] Patankar SV. *Numerical heat transfer and fluid flow. Series in Computational Method in Mechanics and Thermal Sciences*. Mac Graw hill; 1980.
[27] Bouazizi L, Turki S. Numerical Simulation of Flow and Heat Transfer of Nanofluid around a Heated Square Cylinder. *Journal of Applied Fluid Mechanics.* 2016;9(3): 1491-1501.
[28] Singh AK. Thermal conductivity of nanofluids. *Defence Science Journal.* 2008;58(5): 600-607.

## THE AUTHORS

**Bouazizi L.**
e-mail: lot.bouazizi@yahoo.fr
ORCID: 0000-0001-7843-4616

**Turki S.**
e-mail: said.turki@fss.rnu.tn
ORCID: 0000-0003-4468-4259